SPECTROSCOPIC STUDIES OF AGGREGATION AND AUTOXIDATION PROPERTIES OF THE POLYENE ANTIBIOTIC AMPHOTERICIN B

Shirley Schreier*
Department of Biochemistry - Institute of Chemistry - University of São Paulo - C.P. 20780 - 01498-970
M. Teresa Lamy-Freund
Department of Experimental Physics - Institute of Physics - University of São Paulo - C.P. 20516 - 01498-970 - SP - Brazil

A review of the recent work from the Molecular Biophysics Laboratory, at the Institute of Chemistry, University of São Paulo, on the polyene antibiotic amphotericin B (AB) is presented. The studies focus on aggregation and autoxidation properties of the antibiotic. Aggregates were characterized making use of spectroscopic techniques such as electronic absorption, circular dichroism (CD), electron spin resonance (ESR) and quasielastic light scattering (QELS). Autoxidation was monitored by ESR (nitroxide spin label signal loss and spin adduct formation), and by oxygen consumption. AB aggregates formed in DMSO-containing buffer, as well as by complexation with borax, and in the presence of deoxycholate (DOC), were investigated. AB:DOC systems (1:2, molar basis) were found to be polydisperse and unstable. Above the DOC critical micelle concentration (cmc), large mixed AB:DOC aggregates (~5x10^6 Da) coexist with pure DOC micelles. The AB:DOC molar ratio and the micellar DOC concentration vary with concentration. Below the DOC cmc, pure DOC micelles disappear and the mixed aggregates lose DOC, becoming larger and less soluble. The autoxidation process takes place via a radical mechanism and the kinetics depend on the state of AB aggregation. The understanding of these processes should help in the design of more effective and less toxic AB preparations.

Keywords: amphotericin B; polyene antibiotic; aggregation; autoxidation; bile salt; deoxycholate; drug carrier; drug delivery; electron spin resonance; circular dichroism; quasielastic light scattering.

INTRODUCTION

The polyene antibiotic amphotericin B (AB) is widely used in the treatment of systemic mycotic infections. Its use has increased in the past decade due to the rise in the number of immunosupressed patients (especially due to AIDS, leukemia and transplants). AB is very toxic, a major effect being nephrotoxicity.

AB is a polyenic macrocycle containing seven conjugated double bonds (Figure 1). Due to its hydrophobicity and zwitterionic character, AB is very poorly soluble in aqueous medium (ca. 10^{-7} M). In view of this low solubility, AB is currently administered intravenously in the form of a deoxycholate(DOC) complex (1:2, mole:mole, AB:DOC, Fungizone)

AB acts at the membrane level[1-3]. The antibiotic has been proposed to interact with sterols (showing a preference for ergosterol, present in fungi, over cholesterol, present in mammalian hosts), leading to pore formation and increased cell permeability[1-3]. Studies with model lipid membranes have provided evidence for this mechanism[4-7]. Nevertheless, membrane permeability also increased upon addition of AB to phospholipids, in the absence of sterols[7-10]. More recent research has suggested the involvement of oxidative processes in AB's mechanism of action[11,12].

In an attempt to decrease AB's toxic effects, research has been carried out on carriers other than DOC. A large amount of work has been done with phospholipid bilayers and other phospholipid aggregates[13-16]. Some of these preparations have been used in clinical trials[17-19]. Lipoproteins[20] and emulsions[21-23] have also been tested. A recent paper describes the use of triglyceride-rich emulsions[24]. The rationale for the choice of the latter system is based on the ability of these emulsions to bind the apoproteins from endogenous lipoproteins in the circulation; as a result, these particles behave

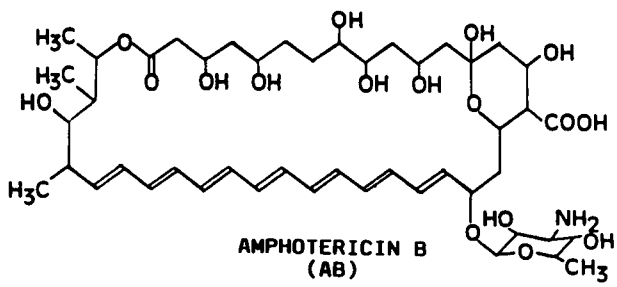

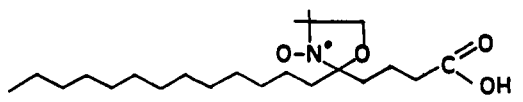

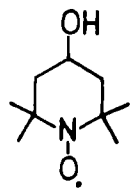

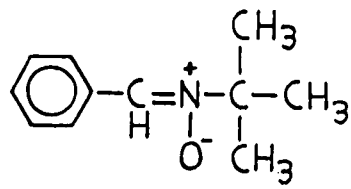

Figure 1. Structures of amphotericin B, 5-doxyl stearic acid, TEMPOL (2,2,6,6-tetramethyl-4-hydroxyl-1-oxyl piperidine), and PBN (phenyl-t-butyl nitrone).

metabolically like native lipoproteins and their contents are internalized via cell surface receptors[25].

It is worthwhile noticing that, in spite of its hydrophobicity, AB does not partition into lipid bilayers to a very large extent when added from the aqueous phase[26]. This is due to the very low solubility of the antibiotic in water, which imposes membrane saturation at low AB concentration in the membrane. Preparations where higher AB:phospholipid molar ratios have been achieved, were obtained by mixing the components prior to bilayer formation[16,26,27]. This variable behavior points at the metastability of such systems. Such metastability is also a consequence of AB's low water solubility which, ultimately, tends to lead to precipitation. Indeed, Lamy-Freund et al[28] have observed that AB:DOC preparations separate out into precipitated AB and DOC in the aqueous phase upon standing for several days.

Clearly, the understanding at a molecular level, of AB's aggregation properties and of its interaction with different carriers should provide useful information for the design of less toxic, specifically targeted preparations.

Our laboratory has been engaged in the study of the AB:DOC system making use of spin labeling electron spin resonance (ESR), electronic absorption, circular dichroism (CD), and quasielastic light scattering (QELS) measurements.

In addition, using spin labels, spin traps, and measurements of oxygen consumption, we have examined the autoxidation of AB, as well as the influence of its aggregation properties on this process.

SPIN LABEL STUDIES OF AGGREGATION PROPERTIES OF THE AB:DOC SYSTEM

When the spin label 5-doxyl stearate (Figure 1) is intercalated in AB:DOC, a two-component ESR spectrum is observed (Figure 2a), one due to strongly immobilized (S) and another due to weakly immobilized (W) probe. As the AB:DOC concentration decreases, W disappears (Figure 2c).

The ESR spectra of 5-doxyl stearate incorporated in pure DOC micelles are those of a weakly immobilized probe (Figure 2d). As the DOC concentration decreases, a spectrum due to probe in the aqueous phase is observed (Figure 2e), and finally, below DOC's critical micellar concentration (cmc), only this latter spectrum, which is due to probe in the aqueous phase, is seen (Figure 2f).

Spectral subtractions (spectrum 2c minus spectrum 2a) indicate that the weakly immobilized component in the two-component spectra of AB:DOC corresponds to pure DOC micelles (dashed line in Figure 2d). The percentages of W in the spectra of 5-doxyl stearate for various AB:DOC concentrations are given in Table I.

Table I. Quantitative analysis of the AB:DOC system as a function of dilution.

[AB] (mM)	Total [DOC] (mM)	%W (±5)	[micellar + monomeric DOC] (mM)	[DOC in the mixed aggregate] (mM)	DOC/AB molar ratio in the mixed aggregates
10.0	20.0	50	6.0	14.0	1.4
5.0	10.0	50	3.0	7.0	1.4
3.0	6.0	40	1.8	4.2	1.4
2.0	4.0	25	1.5	2.5	1.2
1.8	3.6	17	1.5	2.1	1.2
1.6	3.2	11	1.4	1.8	1.1
1.4	2.8	4	1.2	1.6	1.1
1.2	2.4	3	1.2	1.2	1.0
1.0	2.0	0	1.0	1.0	1.0

In order to check whether the strongly immobilized component was due to pure AB or to AB:DOC particles, spectrum 2c was compared to that obtained for 5-doxyl stearate in pure AB. It was found that the separation between the outer extrema in the latter spectrum is 66.5 G whereas it is 63.5 G for AB:DOC, suggesting that, in this system, the strongly immobilized component corresponds to particles that contain both

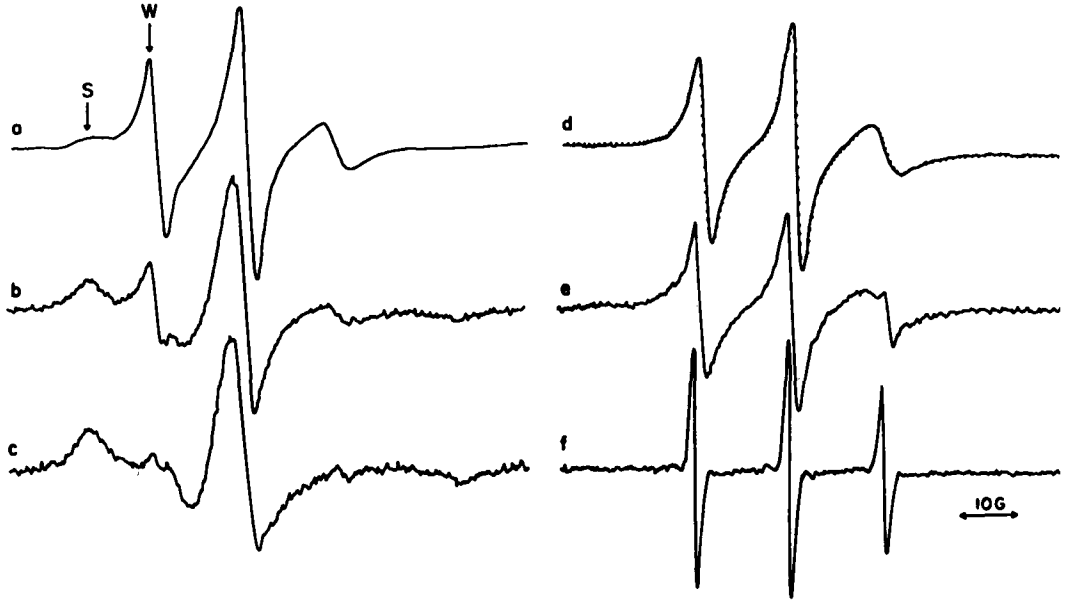

Figure 2. ESR spectra of 5-doxyl stearate in AB:DOC (a-c) and DOC (e-f) systems: (a) 5.0; (b) 1.6; (c) 1.2 mM AB; (d) 6.0; (e) 2.0; (f) 1.0 mM DOC. S and W indicate the low-field components of the spectra due to strongly and weakly immobilized label populations, respectively. The dotted line in d corresponds to the spectrum obtained by subtracting 2c from 2a. NaCl-37 mM phosphate buffer, 300 mOsm, pH 7.4. From ref. 29.

the antibiotic and the bile salt.

Therefore, in the AB:DOC system, particles containing both AB and DOC coexist with pure DOC micelles. As the preparation is diluted to concentrations below the cmc of the bile salt, the micelles of pure DOC disappear, leading to the disappearance of the weakly immobilized component (Figure 2c). As a result, the AB:DOC mixed aggregates lose DOC and the DOC/AB molar ratio decreases in these particles (a more detailed discussion is presented in the next section). The loss of the solubilizing agent leads to larger, less soluble particles, as evinced by filtration, centrifugation and QELS experiments.

When preparations containing AB:DOC (at concentrations ranging from 10 to 1 mM AB) and 5-doxyl stearate are filtered and their ESR spectra taken, before and after filtration through 200 nm filters, the two-component spectrum displayed by the higher concentrations is recovered after filtration (Figure 3). For lower concentrations, the weakly immobilized component disappears and the particles giving rise to the strongly immobilized component are retained in the filters.

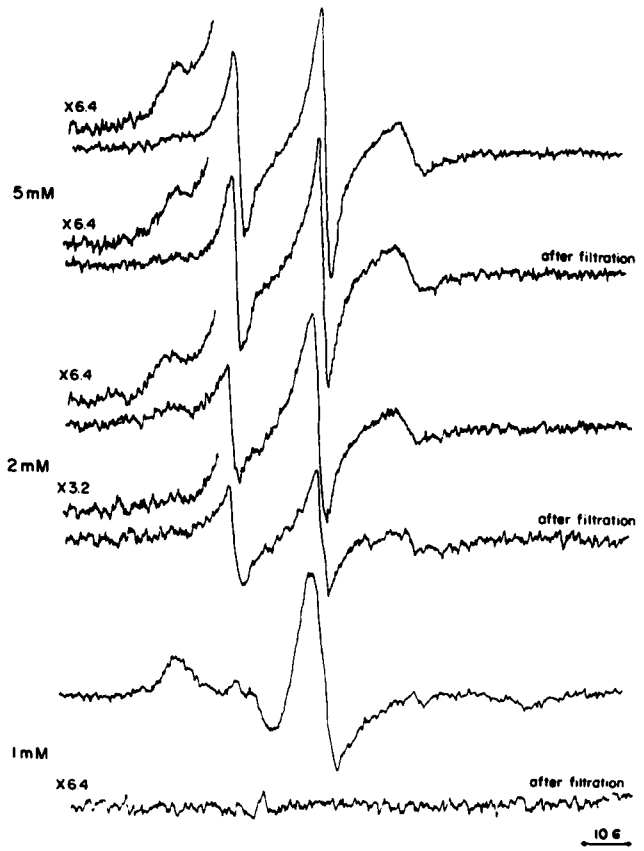

Figure 3. ESR spectra of 5-doxyl stearate in AB:DOC preparations containing 5.0 (top), 2.0 (middle) and 1.0 mM (bottom) amphotericin B, before and after filtration through 220 nm filters. Experimental conditions as in Figure 2. From ref. 29.

These results are corroborated by centrifugation experiments. While large amounts of AB are recovered in the supernatant at 5.0 and 3.0 mM AB (93 and 41%, respectively), only small amounts are recovered at 2.0 and 1.0 mM AB (16 and 2%, respectively), clearly indicating an increase in particle size.

AB:DOC molar ratios in the mixed aggregates as a function of AB and DOC concentration were calculated making use of the following assumptions: 1- the spin probe 5-doxyl stearate partitions between the various aggregates showing no preference for either AB:DOC or micellar DOC; 2- DOC micelles behave similarly in the presence and in the absence of AB:DOC mixed aggregates; 3- when DOC micelles disappear, the spin probe is incorporated in the mixed aggregates. Table I presents the molar ratios in the AB:DOC aggregates as a function of concentration. Although the values are model dependent, the loss of bile salt upon dilution is clearly seen.

FURTHER CHARACTERIZATION AND TIME-DEPENDENCE STUDIES OF AB:DOC AGGREGATES BY QELS

Additional information about particle size and polydispersity of the AB:DOC preparations was obtained from QELS measurements[28]. The latter also allowed the evaluation of the effect of time on aggregate stability.

QELS experiments indicated that AB:DOC aggregates are unstable, and that their size increases as a function of time. The majority of the studies were done at low ionic strength, since at high salt the rate of increase of particle size was too fast to allow for accurate measurements. Average hydrodynamic diameters, D_H, were calculated from measured diffusion coefficients (D) making use of the Stokes-Einstein equation

$$D_H = kT/3\ \eta D$$

where η is the viscosity.

Figure 4 shows that D_H is concentration and time- dependent, the lower concentrations exhibiting larger size and faster rate of increase of D_H.

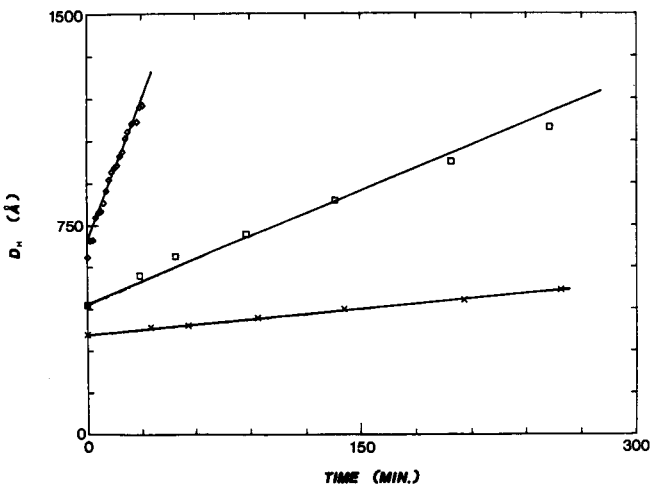

Figure 4. Average hydrodynamic diameter of AB:DOC aggregates as a function of time. 10.0 (X), 5.0 (□), and 2.9 (◇) mM AB. 37 mM phosphate buffer, pH 7.4. From ref. 28.

Figure 5 displays the initial rate of average hydrodynamic diameter change as a function of AB concentration. The right hand scale on the figure indicates the initial rate of D_H change at high ionic strength.

Molecular weights were estimated for the AB:DOC aggregates at several concentrations from the total scattered light at several angles. The initial molecular weight for AB concentrations between 6 and 10 mM was 5×10^6 Da. These values are in rough agreement with those obtained for AB:DOC in hydroalcoholic solution[30].

On the basis of the ESR and QELS results, the AB:DOC system can be envisioned in the following manner: at sufficiently high DOC concentrations, the bile salt exists in the following pseudo equilibria

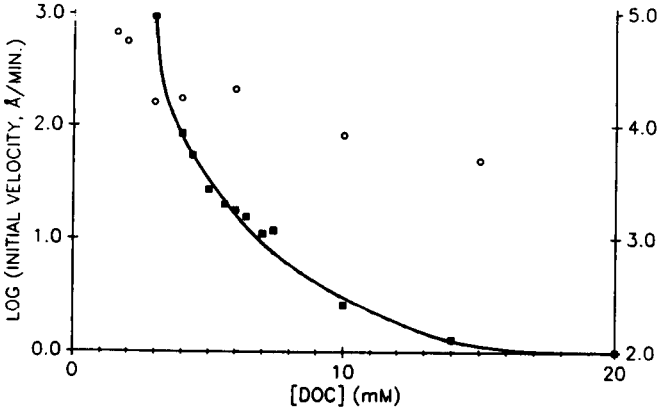

Figure 5. Initial rate of average hydrodynamic diameter change of AB:DOC mixed aggregates as a function of DOC concentration for no added salt (■ ; left hand scale) and in the presence of 83 mM NaCl (○ ; right hand scale). 37 mM phosphate buffer, pH 7.4. From ref. 28.

$$AB_m{:}DOC_n \longleftrightarrow DOC_{monomer} \longleftrightarrow DOC_{micellar}$$

The AB:DOC aggregates are unstable at any initial concentration (Figures 4 and 5). The source of instability is the low AB solubility even in AB:DOC aggregates. DOC, on the other hand, tends towards equilibrium in solution, partitioning itself between monomeric, micellar, and mixed aggregate phases. The m and n subscripts represent the proportion of AB and DOC in mixed aggregates and vary as a function of time and concentration. Upon dilution, the ESR results indicate that the DOC micelles disappear. The disappearance of the micelles is concomitant with the increase in dimensions and decrease in solubility of the AB:DOC aggregates. The results are in quantitative agreement with the observation that DOC is unable to solubilize AB at concentrations below 3.6 mM[31]. Thus, micellar DOC serves as a pool to keep the mixed aggregate in a more soluble form. The disappearance of the micelles leads to loss of DOC from the mixed aggregates.

The behavior of the AB:DOC system is analogous to that found for bile salts-phospholipids systems[32-34]. In the latter case, some regions of the phase diagram also reveal the coexistence of mixed aggregates and pure bile salt micelles.

At micromolar AB concentrations, as found in the circulation, it is conceivable that less DOC remains in association with the antibiotic, as suggested by the different distribution of both compounds in the body of experimental animals[35]. Although significative amounts of AB have been found to be bound to serum proteins[36-38], clearly the state of AB aggregation[39] as well as the interaction between the antibiotic and the carrier system seem to play a role in its toxic properties. Thus, the equilibria between AB in different preparations and serum proteins and cell membranes, and the kinetics of these processes have to be taken into account in the analysis of the mechanism of action and toxicity of AB.

AB AUTOXIDATION: RADICAL FORMATION

AB's seven conjugated double bonds render the molecule prone to autoxidation processes. The spin label 2,2,6,6-tetramethyl-N-oxyl piperidine (TEMPOL) and the spin trap penyl-*t*-butylnitrone (PBN) (Figure 1) were employed to monitor radical formation during AB autoxidation[40]. Loss of TEMPOL ESR signal as a function of time in the presence of AB was observed as a result of the reaction between the formed radicals and the nitroxide moiety.

The signal decay depended both on AB (Figure 6) and TEMPOL (Figure 7) concentrations. The kinetics did not follow any simple rate equation. While the rate of signal decay increased with AB concentration, the opposite was observed for TEMPOL. This latter result is due to the fact that the rate-determining step is the formation of radicals. Since these are formed at a very low steady state concentration, it is easier to detect them when they react with lower spin label concentrations. Indeed, this may be the reason why previous attempts to detect free radicals during polyene antibiotics autoxidation were unsuccessful[41]. On the other hand, free radicals were measured by ESR and have been suggested to be involved in the mechanism of inactivation of polyene antibiotics by Bronov et al[42], in agreement with the early suggestion of Beggs and coworkers, based on the protection of AB's antimycotic activity by antioxidants[43,44]. In more recent work, autoxidation has been proposed to play a role in the mechanism of action of the antibiotic[11,12].

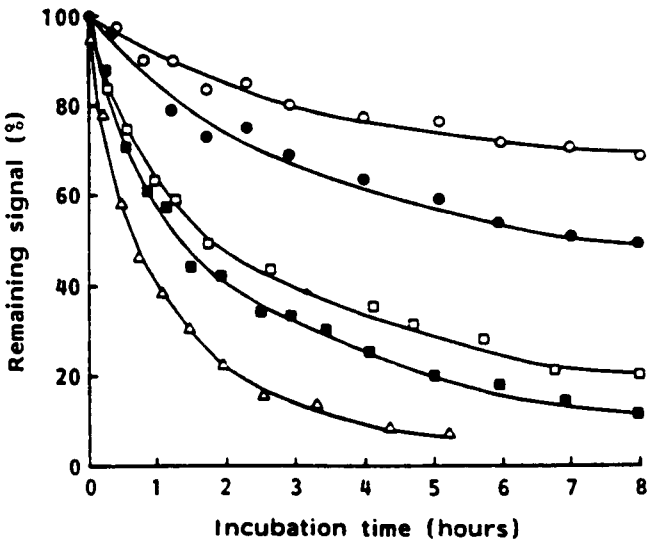

Figure 6. Effect of AB concentration on the kinetics of TEMPOL ESR signal decay in 260 mOsm phosphate buffer - 10% DMSO, pH 7.4. TEMPOL = 5 μM; AB (mM): (○) 1.0; (●) 2.5; (□) 5.0; (■) 7.5; (△) 10.0. From ref. 40.

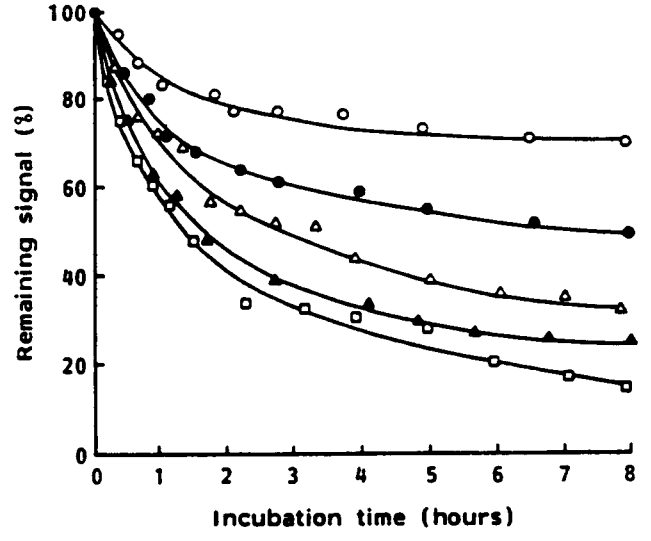

Figure 7. Effect of TEMPOL concentration on the kinetics of TEMPOL ESR signal decay in 260 mOsm phosphate buffer - 10% DMSO, pH 7.4. AB = 5.0 mM. TEMPOL (μM): (○) 25; (●) 10; (△) 7.5; (▲) 5.0; (□) 2.5. From ref. 40.

Free radical formation during AB autoxidation was also monitored with the spin trap PBN. When AB dispersions were prepared in aqueous media containing 10% DMSO (used to dissolve the antibiotic prior to addition of water), the ESR spectra of the spin adducts formed were those of two DMSO radicals (Figure 8c). The hyperfine constants for those spectra are given in Table II; they are very similar to those reported by Saprin and Piette for carbon radicals originating from DMSO[45]. Although this interpretation was questioned by Janzen[46], it seems to apply to our system.

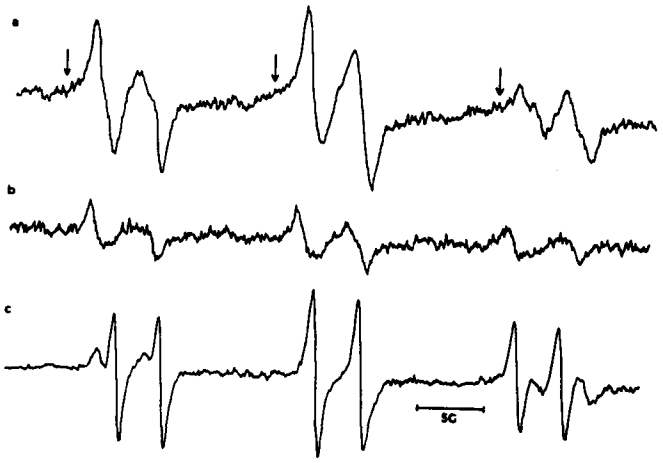

Figure 8. ESR spectra of PBN spin adducts. (a) AB:DOC. The arrows indicate the broader sub-spectrum. (b) AB directly dispersed in 260 mOsm phosphate buffer, pH 7.4. (c) AB in 260 mOsm phosphate buffer - 10% DMSO (v/v), pH 7.4. Spectra were obtained after ca. 20 hours. AB = 10 mM, PBN = 0.1 M. From ref. 40.

Table II. Hyperfine splitting constants of PBN spin adducts.

System	Spectrum	a^N (Gauss)	a^H (Gauss)
AB:DOC (Fig. 8a)		16.10 ± 0.10	3.50 ± 0.10
AB in phosphate	A	15.05 ± 0.05	3.35 ± 0.50
buffer - 10% DMSO			
(Fig. 8c)		15.10[a]	3.42[a]
	B	16.40 ± 0.05	3.70 ± 0.05
		16.46[a]	3.60[a]

[a] Taken from ref. 45.

In order to avoid the use of DMSO, AB:DOC was employed, yielding the composite spectra of Figure 8a. The hyperfine splittings for the narrower subspectrum (Table II) are indicative of a carbon-centered radical. Hyperfine parameters could not be measured for the broader spectrum, which is probably also due to a carbon-centered radical, since the hydrogen hyperfine splitting seems to be similar to that of the narrower spectrum. Both subspectra display differentially broadened lines, indicative of moderately slow tumbling, suggesting that the adducts are located in sites of restricted mobility. The data also suggest that the spin adducts do not correspond to small, water soluble products of AB autoxidation, since such fragments should give rise to narrow lines. These results are in agreement with those of Rickards et al.[41], who have found that the major products of the autoxidation of the polyene antibiotics filipin and lagosin were their epoxides.

Attempts to obtain spin adduct spectra for AB directly dispersed in aqueous medium yielded the results in Figure 8b. The spectrum is very similar to that in Figure 8a. The much lower concentration of spin adduct is due to the very low extent of AB solubilization.

EFFECT OF AGGREGATION ON AB AUTOXIDATION

The kinetics of AB autoxidation were found to depend on the aggregation state of the antibiotic[47]. The aggregates were characterized by optical and CD spectroscopy, and by QELS. Figure 9 presents the optical and CD spectra of monomeric AB (in DMSO) and of AB aggregates in buffer-10% DMSO, in buffer-10% DMSO-100 mM borax, and of AB:DOC.

The various aggregates display different spectra. In DMSO, AB is monomeric. The optical spectrum is typical of the heptaene chromofore, with a resolved vibronic structure. Aggregation takes place for mixtures containing at least 40% buffer, as indicated by a blue shift and concomitant disappearance of the vibronic structure (Figure 9). The intense CD spectra of AB aggregates indicates an organized asymmetric structure. CD spectra of the antibiotic[48] have been interpreted in terms of a helical model[49].

Optical and CD spectra did not reveal differences between

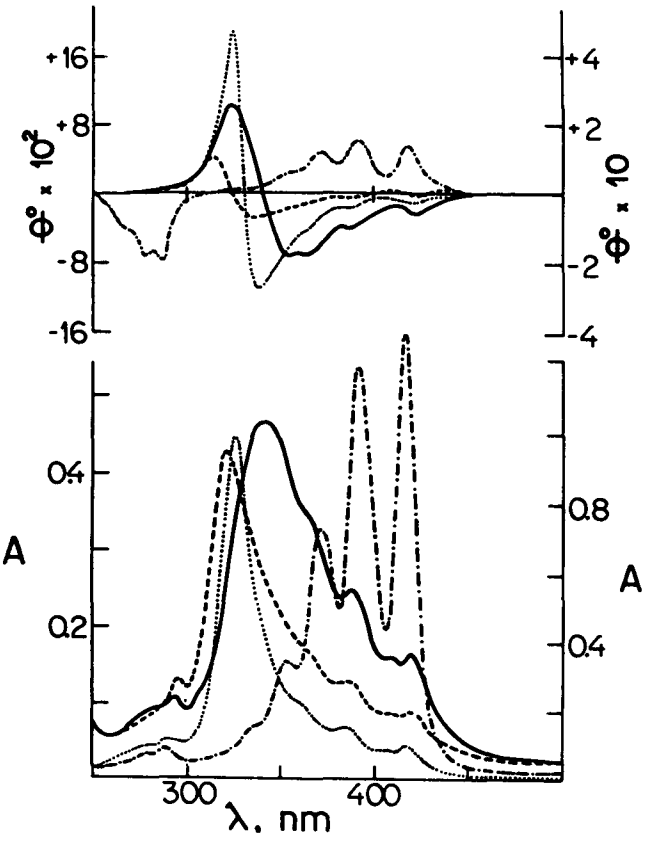

Figure 9. Optical absorption (bottom) and CD (top) spectra of 0.1 mM AB: monomeric in DMSO (-.-.-.-); in buffer-10% DMSO (——); in buffer-10% DMSO-100 mM borax (-----); AB:DOC (...). Path length was 0.1 cm. The right-hand scale corresponds to monomeric AB (bottom) and to AB:DOC (top and bottom). The CD spectrum for monomeric AB is expanded by a factor of 10. From ref. 47.

two different forms of crystalline AB, type I and type II (the former coming from additional purification steps of the latter), in buffer-10% DMSO. Nevertheless, QELS (Table III) and filtration (Table IV) data indicate a difference in aggregate size. Optical and CD spectra arise from the interaction between a few molecules[50,51]. Thus, type I and type II AB

Table III. QELS determination of equivalent hydrodynamic diameter (D_H), polydispersity (Q), and diffusion coefficients (D) of type I and type II AB aggregates and of their borax complexes in water-10% DMSO[a,b]

Medium	AB type	n[c]	D_H, μm	Q	D x 10^{-9}, cm^2/s
Water-10% DMSO	I	15	0.901 ± 0.121	0.369 ± 0.082	3.67 ± 0.73
	II	11	0.275 ± 0.026	0.333 ± 0.054	9.32 ± 2.43
+ 1 mM Borax	I	10	0.215 ± 0.028	0.431 ± 0.106	8.76 ± 4.83
	II	9	0.197 ± 0.014	0.433 ± 0.063	11.55 ± 3.34

[a][AB] = 0.1 mM. [b]The values are mean ± standard error. [c]Number of experiments.

Table IV. Percentage of AB recovered after filtration through membranes of different pore size[a,b].

	AB	
Pore Size, μm	Type I	Type II
1.20	75	84
0.80	55	75
0.45	21	50
0.22	4	16
0.10	2	3

[a][AB] = 0.1 mM in water-10% DMSO. [b]The values are the mean average of three determinations, with a maximum deviation of 10%.

seem to form aggregates of different size, but with similar microenvironments. It is worthwhile to notice that the borax complexes[52] of type I and type II AB have similar dimensions (Table III).

While monomeric type I and type II AB underwent autoxidation at similar rates, their various aggregates displayed different kinetics, as monitored by the loss of the TEMPOL ESR signal (Table V) and by oxygen consumption (Table VI). Since type I and type II AB originate from different stages of

Table V. Time required for loss of 30% TEMPOL ESR signal for different AB preparations[a].

	Time (min) for:	
Medium	Type I AB	Type II AB
Buffer-10% DMSO	18 ± 2 (11)	38 ± 4 (11)
Buffer-10% DMSO + 100 mM borax	35 ± 5 (5)	38 ± 5 (5)
Buffer-10% DMSO + 0.1 mM desferrioxamine	26 ± 1 (2)	46 ± 1 (2)
Pure DMSO	95 ± 6 (5)	98 ± 4 (5)

[a][AB] = 5 mM; [Tempol] = 5 μM; the values are mean ± standard error; the number of experiments is given in parentheses.

purification, their different behavior could arise from impurities that might influence radical formation rather than from different aggregation. To check for spurious metal ion catalysis, two chelating agents were used, diethylenetriamine pentaacetic acid (DTPA) and desferrioxamine[53,54]. DTPA, which chelates transition metal ions nonspecifically[55], had no effect on the kinetics of the TEMPOL signal loss. However, because the DTPA- iron complex also catalyses radical processes[56], desferrioxamine, whose iron complex is considered not to act catalytically[56], was also employed. Table V shows that desferrioxamine inhibits radical formation by type I and type II AB to a similar extent, but the TEMPOL signal loss does not depend on the presence of metal ions (iron) to a large extent, the difference between both types of AB being maintained after the addition of desferrioxamine.

Table VI. Time required for 30% oxygen consumption for different AB preparationsa.

	Time (min) for:	
Medium	Type I AB	Type II AB
Buffer-10% DMSO	40,48	100,120
Pure DMSO	92	90

[a][AB] = 5 mM.

The borax complex of type I AB autoxidizes at a slower rate than the parent compound in buffer (Table V), in agreement with the differences in aggregation observed by electronic absorption and CD spectra (Figure 9) and by QELS (Table III). It is worthwhile noticing that both type I and type II AB borax complexes display similar autoxidation rates, in agreement with the QELS data (Table III), suggesting that both types give rise to similar aggregates upon complexation.

Several interrelated factors, such as oxygen concentration, metal ion content, reaction medium, and aggregation state could influence the rate of AB autoxidation. The above results clearly indicate that aggregation plays a role in the chemical reactivity of the antibiotic.

CONCLUSIONS

The use of spectroscopic techniques such as ESR, CD, optical absorption, and QELS, has provided insight into aggregation properties of systems containing the polyene antibiotic amphotericin B.

AB-deoxycholate preparations were found to be polydisperse, containing both AB:DOC mixed aggregates and pure DOC micelles, above DOC's cmc. The AB:DOC aggregates are large particles whose initial molecular weight is of the order of 5 x 10^6 Da at low ionic strength. Below the cmc of DOC, the mixed aggregates lose the bile salt becoming larger and less soluble. The aggregates are unstable at all concentrations evidencing the tendency of AB to come out of solution due to its low water solubility.

The understanding of the physiochemical basis of AB aggregation and of the metastibily of its aggregates should be of value in the design of less toxic AB preparations.

AB autoxidation was monitored by ESR (loss of nitroxide signal and formation of spin adducts), providing evidence for radical formation, and by oxygen consumption. The results

indicated that aggregation also plays a role in this process, different aggregates yielding different kinetics. Since autoxidation has been implied in the mechanism of action and inactivation of the antibiotic, information regarding the chemistry of this process, as well as knowledge of the effects of AB self or mixed aggregation upon its kinetics should contribute to the development of more effective AB carriers.

REFERENCES

1. Bolard, J.; *Biochim. Biophys. Acta* (1986), **864**, 257.
2. Brajtburg, J.; Powderly, W.G.; Kobayashi, G.; Medoff, G.; *Antimicrob. Agents Chemother.* (1990), **34**, 183.
3. Brajtburg, J.; Powderly, W.G.; Kobayashi, G.; Medoff, G.; *Antimicrob. Agents Chemother.* (1990), **34**, 381.
4. Marty, A.; Finkelstein, A. *J. Gen. Physiol.* (1975), **65**, 515.
5. van Hoogevest, P.; de Kruijff, B.; *Biochim. Biophys. Acta* (1978), **511**, 397.
6. Kasumov, K.M., Borisova, M.P.; Ermishkin, L.N.; Potseluyev, V.M., Silberstein, A.Y.; Vainshtein, V.A.; *Biochim. Biophys. Acta* (1979), **551**, 229.
7. Aracava, Y.; Schreier, S.; Phadke, R.; Deslauriers, R.; Smith, I.C.P.; *Biophys. Chem.* (1981), **14**, 325.
8. Hsu-Chen, C.-C; Feingold, D.S.; *Biochem. Biophys. Res. Commun.* (1973), **51**, 972.
9. Whyte, B.S.; Peterson, R.P.; Harstel, S.C.; *Biochem. Biophys. Res. Commun.* (1989), **164**, 609.
10. Cohen, B.E.; *Biochim. Biophys. Acta* (1992), **1108**, 49.
11. Brajtburg, J.; Elberg, S.; Schwartz, D.R.; Vertut-Croquin, A.; Schlessinger, D.; Kobayashi, G.S.; Medoff, G.; *Antimicrob. Agents Chemother.* (1985), **27**, 172.
12. Sokol-Anderson, M.L.; Brajtburg, J.; Medoff, G.; *J. Infect. Dis.* (1886), **154**, 76.
13. Mehta, R.; Lopez-Berestein, G.; Hopfer, R.; Mills, K..; Juliano, R.L.; *Biochim. Biophys. Acta* (1984), **770**, 230.
14. Szoka, F. C.,Jr.; Milholland, D.; Barza, M.; *Antimicrob. Agents. Chemother.* (1987), **31**, 421.
15. Payne, N.I.; Cosgrove, R.F.; Green, A.P.; Liu, L.; *J. Pharm. Pharmacol.* (1987), **39**, 24.
16. Janoff, A.S.; Boni, L.T.; Popescu, M.C.; Minchey, S.R.; Cullis, P.R.; Madden, T.D.; Taraschi, T.; Gruner, S.M.; Shyamsunder, E.; Tate, M.W.; Mendelsohn, R.; Bonner, D.; *Proc. Natl. Acad. Sci.* U.S.A. (1988), **85**, 6122.
17. Graybill, J.R.; Craven, P.C.; Taylor, R.L.; Williams, D.M.; Magee, W.E.; *J. Infect. Dis.* (1982), **145**, 748.
18. Hospenthal, D.R.; Rogers, A.L.; Beneke, E.S.; *Antimicrob. Agents Chemother.* (1989), **33**, 16.
19. Ringdén, O.; Meunier, F.; Tollemar, J.; Ricci, P.; Tura, S.; Kuse, E.; Viviani, M.A.; Gorin, N.C.; Klastersky, J.; Fenaux, P.; Prentice, H.G.; Ksionski, G.; *J. Antimicrob. Chemother.* (1991), **28** Suppl. B, 73.
20. Koldin, M.H.; Kobayashi, G.S., Brajtburg, J.; Medoff, G.; *Antimicrob. Agents Chemother.* (1985), **28**, 144.
21. Kirsh, R.; Goldstein, R.; Tarloff, J.; Parris, D.; Hook, J.; Hanna, N.; *J. Infect. Dis.* (1988), **158**, 1065.
22. Washington, C.; Taylor, S.J.; Davis, S.S.; *Int. J. Pharm.* (1988), **46**, 25.
23. Illum, L.; West, P., Washington, C.; Davis, S.S.; *Int. J. Pharm.* (1989), **54**, 41.
24. Souza, L.C.; Maranhão, R.C.; Schreier, S.; Campa, A.; *J. Antimicrob. Chemother.* (1993) (in press).
25. Maranhão, R.C.; Tercyak, A.M.; Redgrave, T.G.; *Biochim. Biophys. Acta* (1986), **875**, 247.
26. Aracava, Y.; Smith, I.C.P.; Schreier, S.; *Biochemistry.* (1981), **20**, 5702.
27. Dufourc, E.J.; Smith, I.C.P.; Jarrell, H.C.; *Biochim. Biophys Acta* (1984), **778**, 435.
28. Lamy-Freund, M.T.; Schreier, S.; Peitzsch, R.; Reed, W.F.; *J. Pharm. Sci.* (1991), **80**, 262.
29. Lamy-Freund, M.T.; Ferreira, V.F.N.; Schreier, S.; *Biochim. Biophys. Acta* (1989), **981**, 207.
30. Rinnert, H.; Thirion, C.; Dupont, G.; Lematre, J.; *Biopolymers* (1977), **16**, 2419.
31. Bartner, E.; Zinnes, H.; Moe, R.A.; Kulesza, J.S.; *Antibiotcs Annual* (1957-1958), 53.
32. Mazer, N.A.; Benedek, G.B.; Carey, M.C.; *Biochemistry* (1980), **19**, 601.
33. Lichtenberg, D.; Robson, R.J.; Dennis, E.A.; *Biochim. Biophys. Acta* (1983), **737**, 285.
34. Carey, M.C.; In *Sterols and Bile Salts* (Danielsson, H. and Sjovall, J., eds.), pp. 345-403, Elsevier Science Publishers, Amsterdam, (1980).
35. Lawrence, R.M.; Hoeprich, P.D.; Jagdis, F.A.; Monji, N.; Huston, A.C.; Schaffner, C.P.; *J. Antimicrob. Chemother.* (1981), **6**, 241.
36. Fields, B.T.; Bates, J.H.; Abernathy, R.S.; *Appl. Microbiol.* (1970), **19**, 955.
37. Block, E.R.; Bennett, J.E.; Livoti, L.G.; Klein, W.J.; MacGregor, R.R.; Henderson, L.; *Ann. Int. Med.* (1974), **80**, 613.
38. Brajtburg, J.; Elberg, S.; Bolard, J.; Kobayashi, G.S.; Levy, R.A.; Ostlund, R.E.; Schlessinger, D.; Medoff, G.; *J. Infect. Dis.* (1984), **149**, 986.
39. Bolard, J.; Legrand, P.; Heitz, F.; Cybulska, B.; *Biochemistry* (1991), **30**, 5707.
40. Lamy-Freund, M.T.; Ferreira, V.F.N.; Schreier, S.; *J. Antibiotics* (1985), **38**, 753.
41. Rickards, R.W.; Smith, R.M. and Golding, B.T.; *J. Antibiotics* (1970), **23**, 603.
42. Bronov, L.V.; Kolosova, O.M.; Kroshilova, T.M.; Ivanov, G.C.; Krunchak, V.G.; Komarov, E.V; Fradkova, T.A.; *Antibiotiki* (1982), **22**, 585.
43. Andrews, F.A.; Beggs, W.H.; Sarosi, G.A.; *Antimicrob. Agents Chemother.* (1977), **11**, 615.
44. Andrews, F.A.; Sarosi, G.A.; Beggs, W.H.; *J. Antimicrob. Chemother.* (1979), **5**, 173.
45. Saprin, A.N. and Piette, L.H.; *Arch. Biochem. Biophys.* (1977), **180**, 480.
46. Janzen, E.G.; In *Free Radicals in Biology* (Pryor, W.A., ed.) Vol. IV, pp. 115-154, Academic Press, New York, (1980).
47. Lamy-Freund, M.T.; Ferreira, V.F.N.; Faljoni-Alário, A.; Schreier, S.; *J. Pharm. Sci* (1993), **82**, 162.
48. Ernst, C.; Grange, J.; Rinnert, H.; Dupont, G.; Lematre, J.; *Biopolymers* (1981), **20**, 1575.
49. Hemenger, R.P.; Kaplan, T.; Gray, L.J.; *Biopolymers* (1983), **22**, 911.
50. Mazerski, J.; Bolard, J.; Borowski, E.; *Biochim. Biophys. Acta* (1982), **179**, 11.
51. Mazerki, J.; Grzybowska, J.; Borowski, E.; *Eur. Biophys. J.* (1990), **18**, 159.
52. Strauss, G.; Kral, F.; *Biopolymers* (1982), **21**, 459.
53. Gutteridge, J.M.C.; Richmond, R.; Halliwell B.; *Biochem. J.* (1979), **184**, 469.
54. Graf, E.; Mahoney, J.R.; Bryant, R.G., Eaton, J.W.; *J. Biol. Chem.* (1984), **259**, 3620.
55. Chaberek, S., Frost, A.E., Doran, M.A., Bicknell, N.J.; *J. Inorg. Nucl. Chem.* (1959), **11**, 184.
56. Geep, P.; Davison, A.J.; *Biochim. Biophys Acta*, (1985), **838**, 183.

This special issue of Química Nova is dedicated to Prof. G. Cilento on the occasion of his 70th birthday and is financed by the Fundação de Amparo à Pesquisa do Estado de São Paulo (FAPESP).